PERGAMON

International Journal of Heat and Mass Transfer 44 (2001) 63–72

International Journal of HEAT and MASS TRANSFER

www.elsevier.com/locate/ijhmt

Inverse radiation problem of sources and emissivities in one-dimensional semitransparent media

L.H. Liu*, H.P. Tan, Q.Z. Yu

School of Energy Science and Engineering, Harbin Institute of Technology, 92 West Dazhi Street, Harbin, Heilongjiang Province 150001, People's Republic of China

Received 12 October 1999; received in revised form 26 February 2000

Abstract

An inverse analysis is presented for simultaneous estimation of the source term distribution and the boundary emissivity for an absorbing, emitting, anisotropic scattering, and gray plane–parallel medium with opaque and diffuse bounding surfaces from the knowledge of the exit radiation intensities and temperature at boundary surfaces. The inverse problem is formulated as an optimization problem that minimizes the errors between the exit radiation intensities calculated and the experimental data. The conjugate gradient method and the two-dimensional network searching method are used to solve the inverse problem. The effects of the measurement errors, anisotropic scattering, single-scattering albedo, optical thickness, and boundary emissivity on the accuracy of the inverse analysis are investigated. The results show that the source term and the boundary emissivity can be simultaneously estimated accurately for exact and noisy data, and the estimation of boundary emissivity is more sensitive to the measurement errors.

Keywords: Inverse radiation problem; Radiation source term; Emissivity; Conjugate gradient method; Network searching method

1. Introduction

Radiative heat transfer is important in high temperature devices such as combustion chambers and furnaces. In direct radiation problems, the source term or the temperature distribution of medium, the radiative properties of medium, and the boundary conditions are given, and the radiation intensities are to be determined. On the other hand, in inverse radiation problems, either the radiative properties, or the source term, or the boundary conditions are to be determined from the knowledge of the measured data. The inverse analysis of radiation in a participating medium has a broad range of engineering applications, for example, the remote sensing of the atmosphere, the determination of the radiative properties of medium, and the prediction of temperature distribution in flame, and so on.

Inverse radiation problems that deal with the prediction of the temperature distribution or source term in a medium from radiation measurements have been reported by many researchers. Yi et al. [1], Li and Ozisik [2], Li [3–5], Sewert [6–8] and Liu et al. [9,10] have reconstructed the temperature profiles or source terms in plane–parallel, spherical, cylindrical, and rectangular media by inverse radiation analysis from the data of the radiation intensities exiting the boundaries. Most of the work assumed that the bounding surface is transparent or

* Corresponding author. Tel.: +86-451-641-4315; fax: +86-451-622-1048.

E-mail address: tanhp@etp4.hit.edu.cn (L.H. Liu).

0017-9310/01/$ - see front matter
PII: S0017-9310(00)00081-8

Nomenclature

$\mathbf{a}$	$= (a_1, a_2, \ldots, a_{N-1})^{\mathrm{T}}$
a_n	expansion coefficients of the source term
b	coefficient of interpolation polynomial
$\mathbf{d}$	direction of descent
G	minimum value of objective function for the given ε_0 and ε_{L}
g	scattering asymmetric parameter
I	radiation intensity
S	source term
S_{av}	averaged value of source term
T	temperature
Y	measured exit radiation intensities at the surface, $\tau = 0$
Z	measured exit radiation intensities at the surface, $\tau = \tau_{\mathrm{L}}$

Greek symbols

α	step size
β	conjugate coefficient
Γ	objective function
γ	measurement error of exit radiation intensity
δ	a small specified positive number
ε_0	emissivity of bounding surface, $\tau = 0$
ε_{L}	emissivity of bounding surface, $\tau = \tau_{\mathrm{L}}$
η	error of system parameter
ζ	random variable
μ	direction cosine
σ	standard deviation
$\bar{\sigma}$	Stefan–Boltzmann constant
τ	optical thickness variable
τ_{L}	optical thickness of the slab
ω	single-scattering albedo
∇I	sensitivity coefficient vector
$\nabla \Gamma$	gradient of the objective function with respect to $\mathbf{a}$

Subscripts

estimated	estimated value by inverse analysis
exact	exact value
I	optimum point of ε_0 in discrete searching network
J	optimum point of ε_{L} in discrete searching network
m	direction of discrete ordinates

Superscripts

k	kth iteration
opt	global optimum value

the emissivity of the boundary surface is known. On many occasions, however, the bounding surface may be opaque and its emissivity is unknown. For example, the boundary emissivities of the combustion chamber change with the operating condition, and hence, the unknown temperature profile or source term needs to be estimated simultaneously with the unknown emissivities of the boundary surfaces. Only a limited amount of work is available on this topic. Li and Ozisik [11] used the spherical harmonics method and the conjugate gradient method to estimate the source term and reflectivity of boundary surfaces in an absorbing, emitting, and isotropic scattering plane–parallel media. Liu et al. [12] used the discrete ordinates method and the conjugate gradient method to recover the source term and the emissivities of bounding surfaces in an absorbing, emitting, and non-scattering plane–parallel media. Both of these two works omitted the emission of boundary. In many engineering applications, the emission of boundary cannot be omitted, and the inverse analysis will meet the minimum problem of multimodal function.

The inverse radiation problem considered in this paper is concerned with simultaneous estimation of the source term distribution and the emissivities of bounding surfaces for an absorbing, emitting, anisotropic scattering, and gray one-dimensional semitransparent slab with opaque and diffuse bounding surfaces from the knowledge of the exit radiation intensities at boundary surfaces. In addition, the temperature of bounding surfaces is assumed to be available and the boundary emission cannot be omitted. The inverse problem is formulated thereby as an optimization problem and solved by using the mixed method of conjugate gradient method and two-dimensional network searching method. Test cases will be presented to discuss the effects of the measurement errors, anisotropic scattering, single-scattering albedo, optical thickness, and boundary emissivity on the accuracy of the inverse analysis.

2. Formulation

As illustrated in Fig. 1, we consider an absorbing, emitting, anisotropic scattering, gray plane–parallel medium of optical thickness τ_{L}, and one-dimensional radiation. The bounding surfaces at $\tau = 0$, $\tau = \tau_{\mathrm{L}}$ are opaque and diffuse. The equation of radiative transfer can be written as [13–15]

$$\mu\frac{\partial I(\tau,\mu)}{\partial\tau}+I(\tau,\mu)=(1-\omega)S(\tau)+\frac{\omega}{2}\int_{-1}^{1}I(\tau,\mu')\Phi(\mu',\mu)\,\mathrm{d}\mu' \quad (1)$$

$$S(\tau)=\frac{\bar{n}^2\bar{\sigma}T^4(\tau)}{\pi} \quad (2)$$

with boundary conditions

$$I(0,\mu)=\varepsilon_0 S(0)+2(1-\varepsilon_0)\int_{-1}^{0}I(0,\mu')\mu'\,\mathrm{d}\mu',\mu>0 \quad (3)$$

$$I(\tau_{\mathrm{L}},\mu)=\varepsilon_{\mathrm{L}}S(\tau_{\mathrm{L}})+2(1-\varepsilon_{\mathrm{L}})\int_{0}^{1}I(\tau_{\mathrm{L}},\mu')\mu'\,\mathrm{d}\mu',\quad \mu<0 \quad (4)$$

where $I(\tau,\mu)$ is the radiation intensity, $S(\tau)$ is the source term, $T(\tau)$ is the temperature, $\bar{n}$ is the refractive index, $\bar{\sigma}$ is the Stefan–Boltzmann constant, ω is the single scattering albedo, τ is the optical thickness variable, $\mu=\cos\theta$ is the direction cosine, $\Phi(\mu',\mu)$ is the scattering phase function, ε_0 and ε_{L} are the emissivities at the boundaries of $\tau=0$ and $\tau=\tau_{\mathrm{L}}$ respectively.

For the inverse problem, the source term and the boundary emissivities are regarded as unknown, but other quantities in Eqs. (1)–(4) are known. In addition, the measured exit radiation intensities on the boundaries and the temperature of boundaries are considered available. In the inverse analysis, the source term and the boundary emissivities are estimated simultaneously by utilizing the measured exit radiation intensities.

The source term $S(\tau)$ in the medium is represented by an N-order polynomial in the optical thickness variable τ as

$$S(\tau)=\sum_{n=0}^{N}a_n\tau^n \quad (5)$$

Using the known temperature data $T(0)$ and $T(\tau_{\mathrm{L}})$ of the bounding surfaces, we can know the sources

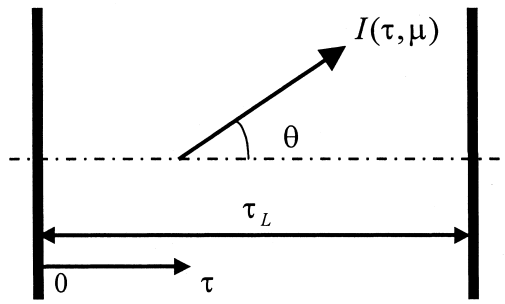

Fig. 1. Schematic of the physical system and coordinates.

$S(0)$ and $S(\tau_{\mathrm{L}})$ at boundaries from Eq. (2), so the source term given by Eq. (5) can be rewritten as [12]

$$S(\tau)=S(0)+\sum_{n=1}^{N-1}a_n\tau^n+\frac{1}{\tau_{\mathrm{L}}^N}\left(S(\tau_{\mathrm{L}})-S(0)-\sum_{n=1}^{N-1}a_n\tau_{\mathrm{L}}^n\right)\tau^N \quad (6)$$

where a_n is the coefficient of the expansion. The coefficients, $a_1, a_2, \ldots, a_{N-1}$, are the parameters to be estimated in the inverse problem. Once the source term is available, the temperature distribution can be determined from the definition given by Eq. (2).

The inverse radiation problem of estimating the unknown source term and boundary emissivities can be formulated as an optimization problem in which the square deviation between the exact radiation intensities calculated and the experiment measurements is minimized. We wish to minimize the object function

$$\Gamma(\mathbf{a},\varepsilon_0,\varepsilon_{\mathrm{L}})=\sum_{\mu_i<0}\left[I(0,\mu_i;\mathbf{a},\varepsilon_0,\varepsilon_{\mathrm{L}})-Y(\mu_i)\right]^2+\sum_{\mu_i>0}\left[I(\tau_{\mathrm{L}},\mu_i;\mathbf{a},\varepsilon_0,\varepsilon_{\mathrm{L}})-Z(\mu_i)\right]^2 \quad (7)$$

where $\mu=\cos\theta$ is the direction cosine; $Y(\mu_i)$ and $Z(\mu_i)$ are the measured exit radiation intensities at the boundary surfaces of $\tau=0$ and $\tau=\tau_{\mathrm{L}}$, respectively; $I(0,\mu_i;\mathbf{a},\varepsilon_0,\varepsilon_{\mathrm{L}})$ and $I(\tau_{\mathrm{L}},\mu_i;\mathbf{a},\varepsilon_0,\varepsilon_{\mathrm{L}})$ are the estimated exit radiation intensities at the boundary surfaces of $\tau=0$ and $\tau=\tau_{\mathrm{L}}$, respectively, for an estimated parameters $\boldsymbol{a}=(a_1,a_2,\ldots,a_{N-1})^{\mathrm{T}}$, ε_0 and ε_{L}.

The objective function $\Gamma(\mathbf{a},\varepsilon_0,\varepsilon_{\mathrm{L}})$ is a multimodal function of variables $\mathbf{a}$, ε_0 and ε_{L}. The method commonly used to solve the minimum point of unimodal function, such as the Newton method and the conjugate gradient method [16], cannot be used directly to minimize the multimodal objective function. Till now there is no general method to solve the global minimum point of multimodal function. In the inverse problem considered in this paper, we discovered that, when the boundary emissivities are given, the object function $\Gamma(\mathbf{a},\varepsilon_0,\varepsilon_{\mathrm{L}})$ is unimodal function of $\mathbf{a}$. Considering this fact, we use the mixed method of the conjugate gradient method and the two-dimensional network searching method. In this method, the entire searching range of ε_0 and ε_{L} is discretized into a series of points $(\varepsilon_{0,i},\varepsilon_{\mathrm{L},j})$. These points form a two-dimensional searching network of ε_0 and ε_{L}. In each discrete point $(\varepsilon_{0,i},\varepsilon_{\mathrm{L},j})$, we use the conjugate gradient method to find the minimum value $G(\varepsilon_{0,i},\varepsilon_{j,\mathrm{L}})$ of $\Gamma(\mathbf{a},\varepsilon_{0,i},\varepsilon_{j,\mathrm{L}})$ at this point. And then we find the minimum value of the sequences $G(\varepsilon_{0,i},\varepsilon_{j,\mathrm{L}})$ and its corresponding values of ε_0 and ε_{L}. Finally, we construct an interpolation function and solve the global minimum point.

3. Method of approach

3.1. Two-dimensional network searching method

The searching procedure consists of following basic steps:

(a) Within the searching range of boundary emissivities, generate sequences with equal interval $\Delta\varepsilon$ as

$$0 = \varepsilon_{0,1} < \varepsilon_{0,2} < \cdots < \varepsilon_{0,i} < \cdots < \varepsilon_{0,M} = 1 \tag{8a}$$

$$0 = \varepsilon_{\mathrm{L},1} < \varepsilon_{\mathrm{L},2} < \cdots < \varepsilon_{\mathrm{L},j} < \cdots < \varepsilon_{\mathrm{L},M} = 1 \tag{8b}$$

and then find the minimum value $G(\varepsilon_{0,i}, \varepsilon_{\mathrm{L},j})$ of object function $\Gamma(\mathbf{a}, \varepsilon_{0,i}, \varepsilon_{\mathrm{L},j})$ in the search point $(\varepsilon_{0,i}, \varepsilon_{\mathrm{L},j})$ by the conjugate gradient method as

$$G(\varepsilon_{0,i}, \varepsilon_{\mathrm{L},j}) = \min_{\mathbf{a}} \Gamma(\mathbf{a}, \varepsilon_{0,i}, \varepsilon_{\mathrm{L},j}) \tag{9}$$

(b) Find the minimum value $G(\varepsilon_{0,I}, \varepsilon_{\mathrm{L},J})$ from the sequence of $G(\varepsilon_{0,i}, \varepsilon_{\mathrm{L},j})$ as

$$G(\varepsilon_{0,I}, \varepsilon_{\mathrm{L},J}) = \min_{i,j} G(\varepsilon_{0,i}, \varepsilon_{\mathrm{L},j}) \tag{10}$$

(c) Based on the point $(\varepsilon_{0,I}, \varepsilon_{\mathrm{L},J}, G(\varepsilon_{0,I}, \varepsilon_{\mathrm{L},J}))$ and its adjacent discrete points, construct an interpolation polynomial, and then find the minimum point $(\varepsilon_0^{\mathrm{opt}}, \varepsilon_{\mathrm{L}}^{\mathrm{opt}})$ of the polynomial. There are three typical cases. In first case, the point $(\varepsilon_{0,I}, \varepsilon_{\mathrm{L},J})$ locates on the one of the four corners of the two-dimensional searching space, i.e., $I = 1$ or $I = M$ and $J = 1$ or $J = M$, the minimum point for the entire searching space of boundary emissivities is $(\varepsilon_{0,I}, \varepsilon_{\mathrm{L},J})$, i.e.,

$$\varepsilon_0^{\mathrm{opt}} = \varepsilon_{0,I} \quad \text{and} \quad \varepsilon_{\mathrm{L}}^{\mathrm{opt}} = \varepsilon_{\mathrm{L},J} \tag{11}$$

In the second case, the point $(\varepsilon_{0,I}, \varepsilon_{\mathrm{L},J})$ locates on the boundaries of the two-dimensional searching space. For example, $I = 1$, $J \neq 1$ and $J \neq M$. In this case, based on the three point $(\varepsilon_{0,1}, \varepsilon_{\mathrm{L},J-1}, G(\varepsilon_{0,1}, \varepsilon_{\mathrm{L},J-1}))$, $(\varepsilon_{0,1}, \varepsilon_{\mathrm{L},J}, G(\varepsilon_{0,1}, \varepsilon_{\mathrm{L},J}))$ and $(\varepsilon_{0,1}, \varepsilon_{\mathrm{L},J+1}, G(\varepsilon_{0,1}, \varepsilon_{\mathrm{L},J+1}))$, construct a two-order interpolation polynomial as

$$G(\varepsilon_{0,1}, \varepsilon_{\mathrm{L}}) = b_0 + b_1\varepsilon_{\mathrm{L}} + b_2\varepsilon_{\mathrm{L}}^2 \tag{12}$$

then find the minimum point $(\varepsilon_0^{\mathrm{opt}}, \varepsilon_{\mathrm{L}}^{\mathrm{opt}})$ as

$$\varepsilon_0^{\mathrm{opt}} = \varepsilon_{0,1} \quad \text{and} \quad \varepsilon_{\mathrm{L}}^{\mathrm{opt}} = -0.5b_1/b_2 \tag{13}$$

In the third case, $(\varepsilon_{0,I}, \varepsilon_{\mathrm{L},J})$ is the inner point of the two-dimensional searching space. We use the point $(\varepsilon_{0,I}, \varepsilon_{\mathrm{L},J}, G(\varepsilon_{0,I}, \varepsilon_{\mathrm{L},J}))$ and its four adjacent points to construct a elliptic paraboloid function as

$$G(\varepsilon_0, \varepsilon_{\mathrm{L}}) = b_0 + b_1\varepsilon_0 + b_2\varepsilon_{\mathrm{L}} + b_3\varepsilon_0^2 + b_4\varepsilon_{\mathrm{L}}^2 \tag{14}$$

then find the minimum point $(\varepsilon_0^{\mathrm{opt}}, \varepsilon_{\mathrm{L}}^{\mathrm{opt}})$ as

$$\varepsilon_0^{\mathrm{opt}} = -0.5b_1/b_3 \quad \text{and} \quad \varepsilon_{\mathrm{L}}^{\mathrm{opt}} = -0.5b_2/b_4 \tag{15}$$

(d) Set $\varepsilon_0 = \varepsilon_0^{\mathrm{opt}}$ and $\varepsilon_{\mathrm{L}} = \varepsilon_{\mathrm{L}}^{\mathrm{opt}}$, find the optimum coefficients $\mathbf{a}^{\mathrm{opt}}$ by the conjugate gradient method from Eq. (7)

$$\Gamma\left(\mathbf{a}^{\mathrm{opt}}, \varepsilon_0^{\mathrm{opt}}, \varepsilon_{\mathrm{L}}^{\mathrm{opt}}\right) = \min_{\mathbf{a}} \Gamma\left(\mathbf{a}, \varepsilon_0^{\mathrm{opt}}, \varepsilon_0^{\mathrm{opt}}\right) \tag{16}$$

3.2. Conjugate gradient method of minimization

The minimization of the objective function with respect to the desired vector is the most important procedure in solving the minimum problem of unimodal function. We use the conjugate gradient method to determine the unknown source term when the boundary emissivities are given. Iterations are built in the following manner [16]:

$$\mathbf{a}^{k+1} = \mathbf{a}^k - \alpha^k \mathbf{d}^k \tag{17}$$

where α^k is the step size, $\mathbf{d}^k$ is the direction vector of descent given by

$$\mathbf{d}^k = \nabla\Gamma^{\mathrm{T}}\left(\mathbf{a}^k, \varepsilon_0, \varepsilon_{\mathrm{L}}\right) + \beta^k \mathbf{d}^{k-1} \tag{18}$$

and the conjugate coefficient β^k is determined from

$$\beta^k = \frac{\nabla\Gamma\left(\mathbf{a}^k, \varepsilon_0, \varepsilon_{\mathrm{L}}\right)\nabla\Gamma^{\mathrm{T}}\left(\mathbf{a}^k, \varepsilon_0, \varepsilon_{\mathrm{L}}\right)}{\nabla\Gamma\left(\mathbf{a}^{k-1}, \varepsilon_0, \varepsilon_{\mathrm{L}}\right)\nabla\Gamma^{\mathrm{T}}\left(\mathbf{a}^{k-1}, \varepsilon_0, \varepsilon_{\mathrm{L}}\right)} \text{ with } \beta^0 = 0 \tag{19}$$

Here, the row vector defined by

$$\nabla\Gamma = \left(\frac{\partial\Gamma}{\partial a_1}, \frac{\partial\Gamma}{\partial a_2}, \ldots, \frac{\partial\Gamma}{\partial a_{N-1}}\right) \tag{20}$$

is the gradient of the objective function. Its components are defined as

$$\frac{\partial\Gamma}{\partial a_n} = 2\sum_{\mu_m<0}\left[I\left(0, \mu_m; \mathbf{a}, \varepsilon_0, \varepsilon_{\mathrm{L}}\right) - Y(\mu_m)\right] \frac{\partial I\left(0, \mu_m; \mathbf{a}, \varepsilon_0, \varepsilon_{\mathrm{L}}\right)}{\partial a_n} + 2\sum_{\mu_m>0}\left[I(\tau_{\mathrm{L}}, \mu_m; \mathbf{a}, \varepsilon_0, \varepsilon_{\mathrm{L}}) - Z(\mu_m)\right]\frac{\partial I(\tau_{\mathrm{L}}, \mu_m; \mathbf{a}, \varepsilon_0, \varepsilon_{\mathrm{L}})}{\partial a_n} \tag{21}$$

In principle, the step size of the kth iteration, α^k, can be determined by minimizing the function, $\Gamma(\mathbf{a}^k - \alpha^k\mathbf{d}^k, \varepsilon_0, \varepsilon_{\mathrm{L}})$, for the given $\mathbf{a}^k$ and $\mathbf{d}^k$ in the following man-

ner:

$$\frac{\partial \Gamma\left(\mathbf{a}^k-\alpha^k\mathbf{d}^k,\,\varepsilon_0,\,\varepsilon_L\right)}{\partial \alpha^k}=0 \tag{22}$$

Since $\Gamma(\mathbf{a}^k-\alpha^k\mathbf{d}^k,\,\varepsilon_0,\,\varepsilon_L)$ is the implicit function of α^k, the exact step size is difficult to be solved. As the first order approximation, we make the first order Taylor expansion of the objective function with respect to α^k. We have from Eq. (22),

$$\begin{aligned}\alpha^k=&\left\{\sum_{\mu_m<0}\left[I\left(0,\,\mu_m;\mathbf{a},\,\varepsilon_0,\,\varepsilon_L\right)-Y(\mu_m)\right]\right.\\&\times\left[\nabla I\left(0,\,\mu_m;\,\mathbf{a},\,\varepsilon_0,\,\varepsilon_L\right)\mathbf{d}^k\right]\\&+\sum_{\mu_m>0}\left[I(\tau_L,\,\mu_m;\,\mathbf{a},\,\varepsilon_0,\,\varepsilon_L)-Z(\mu_m)\right]\\&\left.\times\left[\nabla I(\tau_L,\,\mu_m;\,\mathbf{a},\,\varepsilon_0,\,\varepsilon_L)\mathbf{d}^k\right]\right\}/\\&\left\{\sum_{\mu_m<0}\left[\nabla I\left(0,\,\mu_m;\,\mathbf{a},\,\varepsilon_0,\,\varepsilon_L\right)\mathbf{d}^k\right]^2\right.\\&\left.\times+\sum_{\mu_m>0}\left[\nabla I(\tau_L,\,\mu_m;\,\mathbf{a},\,\varepsilon_0,\,\varepsilon_L)\mathbf{d}^k\right]^2\right\}\end{aligned} \tag{23}$$

where the row vector, ∇I, denotes

$$\nabla I=\left(\frac{\partial I}{\partial a_1},\frac{\partial I}{\partial a_2},\,\ldots,\,\frac{\partial I}{\partial a_{N-1}}\right).$$

3.3. Sensitivity problem

Differentiating Eqs. (1)–(4) with respect to a_n, the equations of sensitivity coefficients can be written as follows:

$$\begin{aligned}&\mu\frac{\partial}{\partial\tau}\left[\frac{\partial I(\tau,\,\mu)}{\partial a_n}\right]+\frac{\partial I(\tau,\,\mu)}{\partial a_n}\\&\quad=(1-\omega)\left[1-\left(\frac{\tau}{\tau_L}\right)^{N-n}\right]\tau^n\\&\qquad+\frac{\omega}{2}\int_{-1}^{1}\frac{\partial I\left(\tau,\,\mu'\right)}{\partial a_n}\Phi\left(\mu',\,\mu\right)\,\mathrm{d}\mu'\end{aligned} \tag{24}$$

with boundary conditions

$$\frac{\partial I(0,\,\mu)}{\partial a_n}=2(1-\varepsilon_0)\int_{-1}^{0}\frac{\partial I\left(0,\,\mu'\right)}{\partial a_n}\mu'\,\mathrm{d}\mu',\quad \mu>0 \tag{25}$$

$$\frac{\partial I(\tau_L,\,\mu)}{\partial a_n}=2(1-\varepsilon_L)\int_{0}^{1}\frac{\partial I\left(\tau_L,\,\mu'\right)}{\partial a_n}\mu'\,\mathrm{d}\mu',\quad \mu<0 \tag{26}$$

for $n=1,\,2,\,\ldots,\,N-1$.

If we take $\partial I/\partial a_n$ for $I(\tau,\,\mu)$, Eqs. (24)–(26) are similar to Eqs. (1)–(4). So the solution procedure of $\partial I/\partial a_n$ is the same as that for the direct problem given by Eqs. (1)–(4), It can be solved by discrete ordinates method S_8 [9,15], and will not be repeated here.

3.4. Stopping criterion

The following condition

$$\left|\Gamma\left(\mathbf{a}^k,\,\varepsilon_0,\,\varepsilon_L\right)-\Gamma\left(\mathbf{a}^{k-1},\,\varepsilon_0,\,\varepsilon_L\right)\right|<\delta \tag{27}$$

is used for terminating the iterative process of $\mathbf{a}$, where δ is a small specified positive number.

3.5. Computational algorithm for the searching of $\mathbf{a}$

We note that the sensitivity coefficient vector ∇I is independent of vector $\mathbf{a}$. The computational algorithm for the searching of $\mathbf{a}$ can be summarized as follows:

Step 1. Pick an initial guess $\mathbf{a}^0$. Set $k=0$.
Step 2. Solve the equations of sensitivity coefficients given by Eqs. (24)–(26), and compute the sensitivity coefficient vector ∇I.
Step 3. Solve the direct problem given by Eqs. (1)–(4), and compute the exit radiative intensities $I(0,\,\mu_m;\,\mathbf{a},\,\varepsilon_0,\,\varepsilon_L)$ and $I(\tau_L,\,\mu_m;\,\mathbf{a},\,\varepsilon_0,\,\varepsilon_L)$.
Step 4. Calculate the objective function $\Gamma(\mathbf{a}^k,\,\varepsilon_0,\,\varepsilon_L)$ given by Eq. (7). Terminate the iteration process if the specified stopping criterion is satisfied. Otherwise, go to Step 5.
Step 5. Compute the gradient of the objective function $\nabla\Gamma$ from Eq. (21).
Step 6. Knowing $\nabla\Gamma$, compute the conjugate coefficient β^k from Eq. (19), then compute the direction vector of descent, $\mathbf{d}^k$, from Eq. (18).
Step 7. Knowing ΔI, $I(0,\,\mu_m;\,\mathbf{a},\,\varepsilon_0,\,\varepsilon_L)$, $I(\tau_L,\,\mu_m;\,\mathbf{a},\,\varepsilon_0,\,\varepsilon_L)$, $Y(\mu_m)$ and $Z(\mu_m)$, compute the step size α^k from Eq. (23).
Step 8. Knowing α^k and $\mathbf{d}^k$, compute the new estimated vector $\mathbf{a}^{k+1}$ from Eq. (17).
Step 9. Set $k=k+1$, and go back to Step 3.

4. Results and discussion

To examine the effectiveness of the method presented in this paper, three different test cases are considered. In the first case, the effects of measurement errors on the estimation of source term and boundary emissivities are considered. In the second case, it is assumed that the relating system parameters such as single-scattering albedo, scattering asymmetry parameter, wall emissivity, and the optical thickness of

slab do not have errors. The effects of these system parameters on the estimation are examined. In the third case, considering that all of the relating system parameters have more or less errors, we analyze the combined effects of the errors of system parameters and the measurement errors on the estimation of source term and boundary emissivities. In all the three cases, the searching space of bounding emissivity is discretized into uniform grids with spacing $\Delta\varepsilon$.

To demonstrate the effects of measurement errors on the predicted source term and boundary emissivities, we consider the random errors. The simulated measured exit radiation intensities with random errors are obtained by adding normally distributed errors into the exact exit radiation intensities on the boundaries as

$$\left[Y(\mu_m)\right]_{\text{measured}} = \left[Y(\mu_m)\right]_{\text{exact}} + \sigma_{Y,\,m}\zeta, \quad \mu_m < 0 \tag{28}$$

$$\left[Z(\mu_m)\right]_{\text{measured}} = \left[Z(\mu_m)\right]_{\text{exact}} + \sigma_{Z,\,m}\zeta, \quad \mu_m > 0 \tag{29}$$

Here, ζ is a normal distributed random variable with zero mean and unit standard deviation. The standard deviations of measured intensities, $\sigma_{Y,\,m}$ and $\sigma_{Z,\,m}$, for a $\gamma\%$ measurement error at 99% confidence, are determined as

$$\sigma_{Y,\,m} = \frac{\left[Y(\mu_m)\right]_{\text{exact}} \times \gamma\%}{2.576} \tag{30}$$

$$\sigma_{Z,\,m} = \frac{\left[Z(\mu_m)\right]_{\text{exact}} \times \gamma\%}{2.576} \tag{31}$$

where 2.576 arises from the fact that 99% of a normally distributed population is contained within ± 2.576 standard deviation of the mean [17].

For the sake of comparison, the root mean square (RMS) error E_{rms} of the estimation for the source term are defined as

$$E_{\text{rms}} = \left\{ \frac{1}{\tau_{\text{L}}} \int_0^{\tau_{\text{L}}} \left[S_{\text{estimated}}(\tau) - S_{\text{exact}}(\tau) \right]^2 \mathrm{d}\tau_{\text{L}} \right\}^{1/2} \tag{32}$$

and the averaged value S_{av} of source term is defined as

$$S_{\text{av}} = \frac{1}{\tau_{\text{L}}} \int_0^{\tau_{\text{L}}} S_{\text{exact}}(\tau)\, \mathrm{d}\tau \tag{33}$$

The scattering phase function is assumed to be linear anisotropic, given as

$$\Phi(\mu, \mu') = 1 + g\mu\mu' \tag{34}$$

Here, g is the scattering asymmetry parameter.

4.1. Case 1

In this case, we first consider two different distributions of source terms expressed as follows:

$$S_1(\tau) = 20 + 500\tau - 1500\tau^2 + 2000\tau^3 - 1000\tau^4 \tag{35}$$

$$S_2(\tau) = 20 + 1687.5\tau - 3375\tau^2 + 3000\tau^3 - 1000\tau^4 \tag{36}$$

The values of system parameters are $\tau_{\text{L}} = 1$, $\omega = 0.5$, and $g = 0.5$, respectively, and the exact emissivities of bounding surfaces are $\varepsilon_{0,\,\text{exact}} = 0.8$ and $\varepsilon_{\text{L},\,\text{exact}} = 0.8$. The grid spacing of the searching network boundary emissivity is $\Delta\varepsilon = 0.1$. Under the condition of no measurement errors, the estimated values of the source terms $S_1(\tau)$ and $S_2(\tau)$ by inverse analysis are shown in Figs. 2 and 3. With no measurement errors, $\gamma = 0\%$, no observable difference could be detected between the estimated and exact values of the source term when the results are presented in graphical form. The estimated boundary emissivities $\varepsilon_{0,\,\text{estimated}} = 0.799$ and $\varepsilon_{\text{L},\,\text{estimated}} = 0.799$, are very close to their exact values.

Finally, we use the simulated experimental data containing random measurement errors of $\gamma = 1\%$ and $\gamma = 3\%$ to estimate the boundary emissivities and the source term $S_3(\tau)$ expressed as a polynomial of degree 4:

$$S_3(\tau) = 15 + 200\tau + 440\tau^2 - 1280\tau^3 + 640\tau^4 \tag{37}$$

The values of system parameters are $\tau_{\text{L}} = 1$, $\omega = 0.3$, and $g = 0.5$, respectively, and the exact emissivities of bounding surfaces are $\varepsilon_{0,\,\text{exact}} = 0.5$ and $\varepsilon_{\text{L},\,\text{exact}} = 0.5$. Different sets of random numbers are used to repeat the inverse calculations. The results of the 20 random samples are shown in Fig. 4. The errors of the source term estimation are within 5% for the

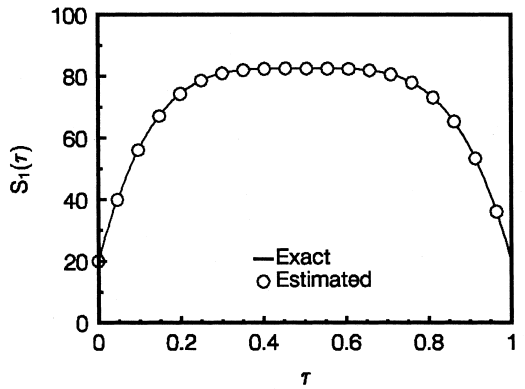

Fig. 2. Estimation of the source term $S_1(\tau)$ with inverse analysis using simulated measured exit radiation intensity data with $\gamma = 0\%$.

case of $\gamma = 1\%$, and 9% for the case of $\gamma = 3\%$. The largest deviations of boundary emissivity estimation are 19% for the case of $\gamma = 1\%$, and 43% for the case of $\gamma = 3\%$, respectively. Clearly, increasing γ from 1 to 3%, decreases the accuracy of the estimation. Even in the case of $\gamma = 3\%$, the estimation of the source term is good. However, the estimation of boundary emissivity is more sensitive to the measurement errors.

4.2. Case 2

We now separately examine the effects of single-scattering albedo ω, scattering asymmetry parameter g, optical thickness τ_L of slab, and boundary emissivity on the accuracy of the inverse estimation. The polynomial $S_1(\tau)$ expressed by Eq. (35) is used as the source term to be estimated. It is assumed that the relating system parameters stated above have no errors, and the exit radiation intensities and the boundary temperature have no measurement errors.

The effects of single-scattering albedo on the estimation of the source term and boundary emissities are shown in Table 1. The values of system parameters are $\tau_L = 1$ and $g = 0.5$. The exact emissivities of bounding surfaces are $\varepsilon_{0,\,\mathrm{exact}} = 0.85$ and $\varepsilon_{L,\,\mathrm{exact}} = 0.85$, and the grid spacing of the searching network of boundary emissivity is $\Delta\varepsilon = 0.1$. As shown in Table 1, increasing ω from 0.0 to 0.9, the accuracy of the estimation decreases. When the single-scattering albedo is less than 0.9, the errors of estimation, $E_{\mathrm{rms}}/S_{\mathrm{av}}$, are less than 4%. The effects of single-scattering albedo on the estimation are not significant.

The effects of scattering asymmetry parameter on the estimation are shown in Tables 2 and 3. The values of system parameters are $\tau_L = 1$ and $\omega = 0.5$. The exact emissivities of bounding surfaces are $\varepsilon_{0,\,\mathrm{exact}} = 0.85$ and $\varepsilon_{L,\,\mathrm{exact}} = 0.85$. The grid spacing of the searching network of boundary emissivity, $\Delta\varepsilon = 0.1$ is used in Table 2, and $\Delta\varepsilon = 0.05$ in Table 3. As shown in Tables 2 and 3, The effects of scattering asymmetry parameter on the estimation are small, especially with $\Delta\varepsilon = 0.05$. Comparing the two tables, we can find that the grid spacing $\Delta\varepsilon$ has influence on the estimation. Decreasing $\Delta\varepsilon$, the accuracy of the estimation will be

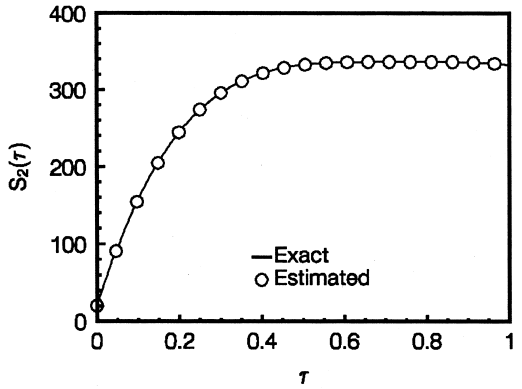

Fig. 3. Estimation of the source term $S_2(\tau)$ with inverse analysis using simulated measured exit radiation intensity data with $\gamma = 0\%$.

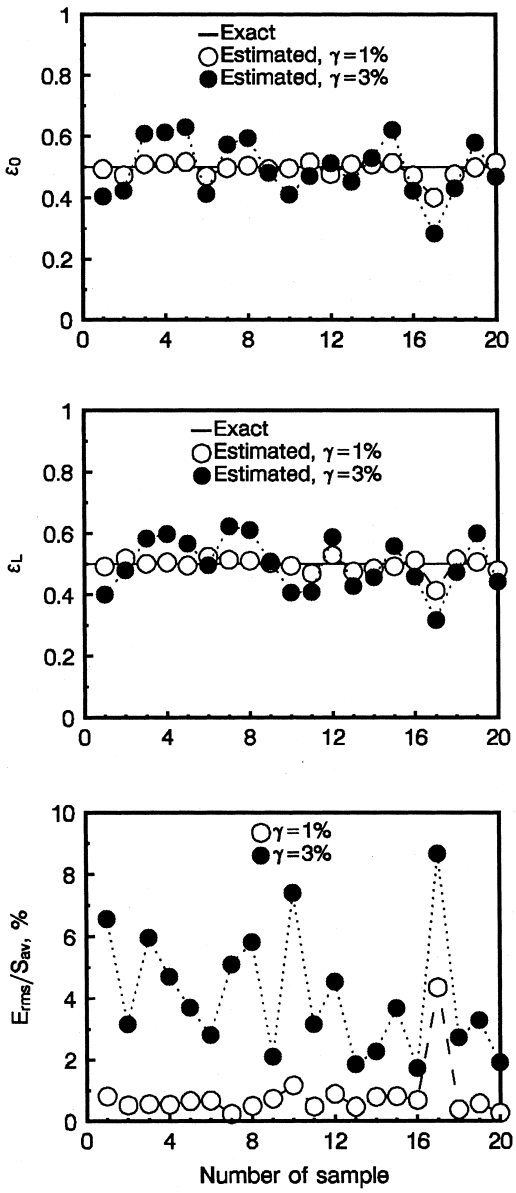

Fig. 4. The effects of the measurement errors of exit radiation intensities on the inverse estimation for the case $\tau_L = 1$, $\omega = 0.3$, $g = 0.5$, and $\Delta\varepsilon = 0.1$.

Table 1
The results of the inverse estimation with different single-scattering albedo ω for the case $\tau_L = 1$, $g = 0.5$, $\varepsilon_{0,\,exact} = 0.85$, $\varepsilon_{L,\,exact} = 0.85$, and $\Delta\varepsilon = 0.1$

ω	$\varepsilon_{0,\,estimated}$	$\varepsilon_{L,\,estimated}$	E_{rms}	E_{rms}/S_{av} (%)
0.00	0.811	0.811	1.059	1.528
0.15	0.810	0.810	1.160	1.674
0.30	0.809	0.809	1.284	1.852
0.45	0.808	0.808	1.450	2.093
0.60	0.808	0.808	1.687	2.434
0.75	0.807	0.807	2.015	2.907
0.90	0.806	0.806	2.549	3.679

improved. However, the computational time will be increase significantly with the decrease of $\Delta\varepsilon$.

The effects of optical thickness on the estimation are shown in Table 4. The values of system parameters are $\omega = 0.5$ and $g = 0.5$. The exact emissivities of bounding surfaces are $\varepsilon_{0,\,exact} = 0.85$ and $\varepsilon_{L,\,exact} = 0.85$. The grid spacing of the searching network of boundary emissivity, $\Delta\varepsilon = 0.1$, is used. As shown in Table 4, the optical thickness has influence on the estimation of source term and boundary emissivity. When the optical thickness is less than 1.0, the errors of the estimation increase with the decrease of the optical thickness. This is because the signals of exit radiation intensities measured on the boundaries are disturbed largely by the emission of bounding surfaces. When the optical thickness is larger than 20.0, the errors of the estimation increase with the optical thickness. This is because the radiation signals of inner layer of the slab are attenuated largely by the layer adjacent to the bounding surface when the signals reach the boundary. However, when the optical thickness τ_L are within the range from 1.0 to 20.0, the errors of the inverse estimation are small.

Table 2
The results of the inverse estimation with different scattering asymmetry parameter g for the case $\tau_L = 1$, $\omega = 0.5$, $\varepsilon_{0,\,exact} = 0.85$, $\varepsilon_{L,\,exact} = 0.85$, and $\Delta\varepsilon = 0.1$

g	$\varepsilon_{0,\,estimated}$	$\varepsilon_{L,\,estimated}$	E_{rms}	E_{rms}/S_{av} (%)
−1.00	0.816	0.816	1.267	1.828
−0.75	0.814	0.814	1.320	1.904
−0.50	0.813	0.813	1.380	1.992
−0.25	0.811	0.811	1.413	2.040
0.00	0.810	0.810	1.455	2.099
0.25	0.809	0.809	1.490	2.150
0.50	0.808	0.808	1.523	2.198
0.75	0.807	0.807	1.557	2.246
1.00	0.806	0.806	1.579	2.279

Table 3
The results of the inverse estimation with different scattering asymmetry parameter g for the case $\tau_L = 1$, $\omega = 0.5$, $\varepsilon_{0,\,exact} = 0.85$, $\varepsilon_{L,\,exact} = 0.85$ and $\Delta\varepsilon = 0.05$

g	$\varepsilon_{0,\,estimated}$	$\varepsilon_{L,\,estimated}$	E_{rms}	E_{rms}/S_{av} (%)
−1.00	0.8498	0.8498	7.582×10^{-3}	1.094×10^{-2}
−0.75	0.8498	0.8498	7.272×10^{-3}	1.049×10^{-2}
−0.50	0.8498	0.8498	1.019×10^{-2}	1.470×10^{-2}
−0.25	0.8488	0.8498	5.348×10^{-3}	7.717×10^{-3}
0.00	0.8498	0.8498	5.570×10^{-3}	8.038×10^{-3}
0.25	0.8497	0.8497	1.013×10^{-2}	1.462×10^{-2}
0.50	0.8497	0.8497	8.316×10^{-3}	1.200×10^{-2}
0.75	0.8497	0.8497	1.102×10^{-2}	1.591×10^{-2}
1.00	0.8497	0.8497	8.725×10^{-3}	1.259×10^{-2}

The influence of boundary emissivity on the inverse estimation is shown in Table 5. The values of system parameters are $\tau_L = 1.0$, $\omega = 0.3$ and $g = 0.5$. The grid spacing of the searching network of boundary emissivity is $\Delta\varepsilon = 0.1$. As shown in Table 5, the errors of the inverse estimation are very small.

4.3. Case 3

In the practical processes of measurement and inverse solution, the known system parameters may have random errors more or less. In order to examine the combined effects of the errors of system parameters and the measurement errors on the inverse estimation, we considered the source term $S_3(\tau)$ expressed by Eq. (37), and assumed that all known system parameters have normally distributed random errors. The random samples are generated in the following manner

Table 4
The results of the inverse estimation with different optical thickness τ_L for the case $\omega = 0.5$, $g = 0.5$, $\varepsilon_{0,\,exact} = 0.85$, $\varepsilon_{L,\,exact} = 0.85$, and $\Delta\varepsilon = 0.1$

τ_L	$\varepsilon_{0,\,estimated}$	$\varepsilon_{L,\,estimated}$	E_{rms}	E_{rms}/S_{av} (%)
0.5	0.805	0.805	6.314	9.112
1.0	0.808	0.808	1.523	2.198
2.0	0.810	0.810	0.527	0.781
5.0	0.816	0.816	0.601	0.868
10.0	0.827	0.827	0.713	1.028
20.0	0.828	0.828	1.104	1.594
30.0	0.738	0.850	5.321	7.640
40.0	0.931	0.943	7.431	10.669

Table 5
The results of the inverse estimation with different boundary emissitivies for the case $\tau_L = 1$, $\omega = 0.3$, $g = 0.5$, $\Delta\varepsilon = 0.1$

$\varepsilon_{0,\text{exact}}$	$\varepsilon_{L,\text{exact}}$	$\varepsilon_{0,\text{estimated}}$	$\varepsilon_{L,\text{estimated}}$	E_{rms}	E_{rms}/S_{av} (%)
0.0	0.0	0.000	0.000	4.497×10^{-4}	6.489×10^{-4}
0.1	0.1	0.099	0.099	4.534×10^{-2}	6.542×10^{-2}
0.2	0.2	0.199	0.199	4.233×10^{-2}	6.109×10^{-2}
0.3	0.3	0.299	0.299	3.686×10^{-2}	5.320×10^{-2}
0.4	0.4	0.399	0.399	4.009×10^{-2}	5.784×10^{-2}
0.5	0.5	0.499	0.499	3.627×10^{-2}	5.235×10^{-2}
0.6	0.6	0.599	0.599	3.570×10^{-2}	5.151×10^{-2}
0.7	0.7	0.699	0.699	3.246×10^{-2}	4.684×10^{-2}
0.8	0.8	0.799	0.799	3.278×10^{-2}	4.730×10^{-2}
0.9	0.9	0.899	0.899	2.866×10^{-2}	4.135×10^{-2}
1.0	1.0	1.000	1.000	3.934×10^{-3}	5.677×10^{-3}
0.0	1.0	0.000	1.000	1.772×10^{-3}	2.558×10^{-3}
0.1	0.9	0.099	0.899	3.761×10^{-2}	5.427×10^{-2}
0.2	0.8	0.199	0.799	3.537×10^{-2}	5.104×10^{-2}
0.3	0.7	0.299	0.699	3.570×10^{-2}	5.151×10^{-2}
0.4	0.6	0.399	0.599	3.516×10^{-2}	5.074×10^{-2}

$$[\Theta_i] = [\Theta_i]_{\text{exact}} + \sigma_{\Theta_i}\zeta \tag{38}$$

Here, $[\Theta_i]$ represent the optical thickness of slab, the single-scattering albedo, the scattering asymmetry parameter, and the measured data of the source $S(0)$ and $S(\tau_L)$ at boundaries, respectively; $[\Theta_i]_{\text{exact}}$ are the corresponding exact values of these parameters stated above. The standard deviations of these parameters, σ_{Θ_i}, is chosen as

$$\sigma_{\Theta_i} = \frac{[\Theta_i]_{\text{exact}} \times \eta\%}{2.576} \tag{39}$$

Fig 5 shows the results of the inverse estimation for the 20 random samples. The errors of the source term estimation are within 2% for the case of $\gamma = 1\%$ and $\eta = 1\%$, and 5% for the case of $\gamma = 1\%$ and $\eta = 3\%$. The largest deviations of boundary emissivity estimation are 7% for the case of $\gamma = 1\%$ and $\eta = 1\%$, and 22% for the case of $\gamma = 1\%$ and $\eta = 3\%$, respectively. Clearly, increasing η from 1% to 3%, the accuracy of the estimation decreases. Even in the case of $\gamma = 1\%$ and $\eta = 3\%$, the estimation of the source term is good. Comparing with Fig. 4, we note that the errors of the inverse estimation are mainly brought about by measurement errors of the exit radiation intensities. In order to improve the accuracy of the estimation of source term and boundary emissivities, the measurement errors of the exit radiation intensities must be confined to an appropriate limit.

For all cases considered above, calculations are started with an initial guess $\mathbf{a} = 0$. The CPU time required for each sample of estimation calculation varied from 10 to 40 min on a personal computer with an Intel Pentium III 450 MHz processor.

5. Conclusions

An inverse analysis is presented for simultaneous estimation of the source term distribution and the boundary emissivity for an absorbing, emiting, anisotropic scattering, and gray plane–parallel medium with opaque and diffuse bounding surfaces from the knowledge of the exit radiation intensities and temperature at boundary surfaces. The inverse problem is formulated as an optimization problem that minimizes the errors between the exit radiation intensities calculated and the experimental data. The conjugate gradient method and the two-dimensional network searching method are used to solve the inverse problem. The effects of the measurement errors, anisotropic scattering, single-scattering albedo, optical thickness, and boundary emissivity on the accuracy of the inverse analysis are investigated. The results show that the source term and the boundary emissivity can be simultaneously estimated accurately for exact and noisy data, and the estimation of boundary emissivity is more sensitive to the measurement errors. The accuracy of the inverse estimation is limited mainly by the measurement errors of the exit radiation intensities on the boundaries. In order to reduce the errors of the inverse estimation, the measurement errors must be confined to an appropriate limit. The algorithm can be extended to non-gray media.

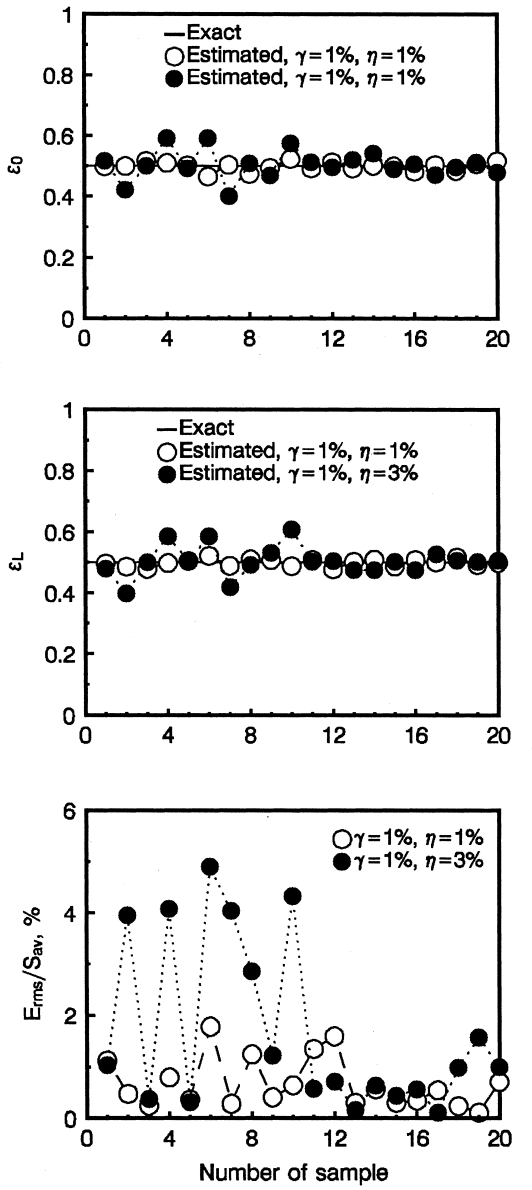

Fig. 5. The combined effects of the errors of system parameters and the measurement errors of exit radiation intensities on the inverse estimation for the case $\tau_L = 1$, $\omega = 0.3$, $g = 0.5$, and $\Delta\varepsilon = 0.1$.

Acknowledgements

The supports of this work by Fok Ying Tung Education Foundation, the National Science Foundation of China, the Chinese National Science Fund for Distinguish Young Scholar, and the Science Fund of Harbin Institute of Technology are gratefully acknowledged.

References

[1] H.C. Yi, R. Sanchez, N.J. McCormick, Bioluminescence estimation from ocean in situ irradiances, Applied Optics 31 (1992) 822–830.
[2] H.Y. Li, M.N. Ozisik, Identification of the temperature profile in an absorbing, emitting, and isotropically scattering medium by inverse analysis, ASME Journal of Heat Transfer 116 (1992) 1060–1063.
[3] H.Y. Li, Estimation of the temperature profile in a cylindrical medium by inverse analysis, Journal Quantitative Spectroscopy Radiative Transfer 52 (1994) 755–764.
[4] H.Y. Li, An inverse source problem in radiative transfer for spherical media, Numerical Heat Transfer 31B (1997) 251–260.
[5] H.Y. Li, Inverse radiation problem in two-dimensional rectangular media, Journal of Thermophysics and Heat Transfer 11 (1997) 556–561.
[6] C.E. Siewert, A new approach to the inverse problem, Journal of Mathematical Physics 19 (1978) 2619–2621.
[7] C.E. Siewert, An inverse source problem in radiative transfer, Journal Quantitative Spectroscopy Radiative Transfer 50 (1993) 603–609.
[8] C.E. Siewert, A radiative-transfer inverse-source problem for a sphere, Journal Quantitative Spectroscopy Radiative Transfer 52 (1994) 157–160.
[9] L.H. Liu, H.P. Tan, Q.Z. Yu, Inverse radiation problem in one-dimensional semitransparent plane–parallel media with opaque and specularly reflecting boundaries, Journal Quantitative Spectroscopy Radiative Transfer 64 (2000) 395–407.
[10] L.H. Liu, H.P. Tan, Q.Z. Yu, Inverse radiation problem of temperature field in three-dimensional rectangular furnaces, International Communications in Heat and Mass Transfer 26 (1999) 239–248.
[11] H.Y. Li, M.N. Ozisik, Inverse radiation problem for simultaneous estimation of temperature profile and surface reflectivity, Journal of Thermophysics and Heat Transfer 7 (1993) 88–93.
[12] L.H. Liu, H.P. Tan, Q.Z. Yu, Simultaneous identification of temperature profile and wall emissivities in semitransparent medium by inverse radiation analysis, Numerical Heat Transfer 36A (1999) 511–525.
[13] M.N. Ozisik, in: Radiative Heat Transfer and Interactions with Conduction and Convection, Wiley, New York, 1973, pp. 249–309.
[14] R. Siegel, J.R. Howell, in: Thermal Radiation Heat Transfer, 2nd ed., Hemisphere, New York, 1981, pp. 463–473.
[15] M.F. Modest, in: Radiative Heat Transfer, McGraw-Hill, New York, 1993, pp. 541–567.
[16] Y.X. Yuan, W.Y. Sun, Optimization Theory and Method, Science Press, Beijing, 1997, pp. 183–199.
[17] M.N. Ozisik, Heat Conduction, 2nd ed., Wiley, New York, 1993, pp. 571–594.